Mol Neurobiol (2016) 53:4529–4538
DOI 10.1007/s12035-015-9386-9

Anti-Vascular Endothelial Growth Factor Treatment Suppresses Early Brain Injury After Subarachnoid Hemorrhage in Mice

Lei Liu[1] · Masashi Fujimoto[1] · Fumihiro Kawakita[1] · Fumi Nakano[1] · Kyoko Imanaka-Yoshida[2,3] · Toshimichi Yoshida[2,3] · Hidenori Suzuki[1,3]

Received: 15 June 2015 / Accepted: 11 August 2015 / Published online: 21 August 2015

Abstract The role of vascular endothelial growth factor (VEGF) in early brain injury (EBI) after subarachnoid hemorrhage (SAH) remains unclear. The aim of this study was to investigate effects of anti-VEGF therapy on EBI after SAH. C57BL/6 male mice underwent sham or filament perforation SAH modeling, and vehicle or two dosages (0.2 and 1 μg) of anti-VEGF antibody were randomly administrated by an intracerebroventricular injection. Neuroscore, brain water content, immunoglobulin G staining, and Western blotting were performed to evaluate EBI at 24–48 h. To confirm the role of VEGF, anti-VEGF receptor (VEGFR)-2 (a major receptor of VEGF) antibody was intracerebroventricularly administered and the effects on EBI were evaluated at 24 h. A higher dose, but not a lower dose, of anti-VEGF antibody significantly ameliorated post-SAH neurological impairments and brain edema at 24–48 h post-SAH. Post-SAH blood-brain barrier disruption was also inhibited by anti-VEGF antibody. The protective effects of anti-VEGF antibody were associated with the inhibition of post-SAH induction of VEGF, VEGFR-2, phosphorylated VEGFR-2, interleukin-1β and a matricellular protein tenascin-C (TNC). Anti-VEGFR-2 antibody also suppressed post-SAH neurological impairments and brain edema associated with VEGFR-2 inactivation and TNC downregulation. These findings demonstrated that VEGF causes post-SAH EBI via VEGFR-2 and TNC and that anti-VEGF therapy is effective for post-SAH EBI.

Keywords Subarachnoid hemorrhage · Vascular endothelial growth factor · Blood-brain barrier · Tenascin-C · Antibody neutralization

Abbreviations

ANOVA	Analysis of variance
BBB	Blood-brain barrier
CSF	Cerebrospinal fluid
EBI	Early brain injury
EGF	Epidermal growth factor
IL	Interleukin
MAPK	Mitogen-activation protein kinase
PBS	Phosphate-buffered saline
PDGF	Platelet-derived growth factor
p-VEGFR-2	Phosphorylated vascular endothelial growth factor receptor-2
SAH	Subarachnoid hemorrhage
TNC	Tenascin-C
VEGF	Vascular endothelial growth factor
VEGFR	Vascular endothelial growth factor receptor
ZO	Zona occludens

Introduction

Subarachnoid hemorrhage (SAH) is a serious life-threatening type of stroke caused by bleeding into the subarachnoid space surrounding the brain. It elicits a wide range of stress

Electronic supplementary material The online version of this article (doi:10.1007/s12035-015-9386-9) contains supplementary material, which is available to authorized users.

✉ Hidenori Suzuki
suzuki02@clin.medic.mie-u.ac.jp

[1] Department of Neurosurgery, Mie University Graduate School of Medicine, 2-174 Edobashi, Tsu, Mie 514-8507, Japan

[2] Department of Pathology and Matrix Biology, Mie University Graduate School of Medicine, Tsu, Japan

[3] Research Center for Matrix Biology, Mie University Graduate School of Medicine, Tsu, Japan

responses in brain tissues and results in brain injury. The term early brain injury (EBI) is a concept to explain pathophysiological changes that occur in brain within 72 h of SAH [1]. The mechanism of post-SAH EBI is complex and involves many pathways, such as hypoxia, molecular alteration, inflammation response, and imbalance of ionic homeostasis, causing cell apoptosis and blood-brain barrier (BBB) disruption [2]. Enhanced BBB permeability promotes immune molecules to enter into brain tissue and aggravates homeostatic imbalance, and the vicious circle may lead to further aggravation of brain injury [1, 2]. Thus, the progress of BBB disruption has a pivotal role during EBI that is induced by SAH.

Vascular endothelial growth factor (VEGF) has a significant role in vascular permeability and angiogenesis during embryonic vasculogenesis and in physiological and pathological angiogenesis in non-neural vessels, and these effects are mediated by VEGF receptor (VEGFR)-2, which is present on endothelial cells [3]. It has also been demonstrated that VEGF enables to enhance BBB permeability in normal mice brain [4] and inflammatory disease of mice brain [5]. Kusaka et al. [6] reported that a Src-family kinase inhibitor reduced BBB permeability, as well as the expression of VEGF and the phosphorylation of mitogen-activation protein kinases (MAPKs) in the cerebral cortex after experimental SAH. However, no studies have investigated effects of the direct blockage of VEGF on EBI or BBB disruption after SAH.

Tenascin-C (TNC) belongs to the extracellular matrix protein family and upregulates during inflammation [7]. It exerts various functions through binding to cell surface receptors, other matrix proteins, and growth factors [7]. Our previous studies reported that TNC concentration in the cerebrospinal fluid (CSF) was increased in SAH patients with worse outcomes [8], and that TNC was implicated in EBI after experimental SAH in rats [9]. In this study, we aimed to investigate if anti-VEGF therapy is effective against post-SAH EBI and if TNC is involved in VEGF-induced EBI.

Materials and Methods

All procedures were approved by the Animal Ethics Review Committee of Mie University, and were carried out according to the institution's Guidelines for Animal Experiments. One hundred and eighty six C57BL/6 male mice (age 10–12 weeks, 25–30 g; SLC, Hamamatsu, Japan) were used, maintained on a constant 12-h light/12-h dark cycle in a temperature- and humidity-controlled room, and given ad libitum access to feed and water.

Experimental SAH Model and Study Protocol

The endovascular filament perforation SAH model was produced as previously described [10]. Briefly, mice were anesthetized with intraperitoneal tribromoethanol (250 μg/g body weight). The left common, internal and external carotid arteries were exposed, and a sharpened 4–0 monofilament nylon suture was advanced rostrally into the left internal carotid artery about 15 mm from the external carotid artery stump to perforate the bifurcation of the left anterior and middle cerebral arteries. The filament was advanced 3 mm into the left internal carotid artery without perforating the artery for sham operation. Blood pressure and heart rate were noninvasively monitored during operation from the tail. Mice rectal temperature was kept at 37 °C during surgery. After the surgery, 1 mL of normal saline was injected subcutaneously to prevent dehydration, and then the mice were returned to the clean cages and kept the room temperature at 25±1 °C.

First, to evaluate the effect of anti-VEGF antibody treatment, mice were randomly divided into five groups: sham+vehicle (n=24), sham+1 μg anti-VEGF antibody (n=18), SAH+vehicle (n=35), SAH+0.2 μg anti-VEGF antibody (n=11) and SAH+1 μg anti-VEGF antibody (n=34) groups. The vehicle or antibody was intracerebroventricularly administrated after 30 min of operation. Neurological score, SAH severity, and brain water content were evaluated at 24 and 48 h, and BBB permeability and Western blotting of VEGF, VEGFR-2, phosphorylated VEGFR-2 (p-VEGFR-2), and TNC were assessed at 24 h post-operation. To exclude the possibility of a nonspecific response to intracerebroventricular protein injection, 1 μg normal goat immunoglobulin G (IgG; Abcam, Cambridge, MA) was also injected as an isotype control, and the effect on neuroscore, SAH severity, and brain water content were evaluated at 24 h.

Secondly, to confirm the role of VEGF in EBI, effects of a selective inhibition of VEGFR-2, a major receptor of VEGF, were evaluated. Mice were randomly divided into four groups: sham+vehicle (n=12), sham+2 μg anti-VEGFR-2 antibody (n=12), SAH+vehicle (n=17), and SAH+2 μg anti-VEGFR-2 antibody (n=17) groups. The vehicle or antibody was intracerebroventricularly administrated at 30 min post-operation. After 24 h, neurological score, brain water content, and Western blotting of VEGFR-2, p-VEGFR-2, and TNC were evaluated.

Intracerebroventricular Injection

An intracerebroventricular injection was performed by a modification of the method previously described [10]. Mice were placed in a stereotactic head holder and the needle of a 2 μL Hamilton syringe (Hamilton Company, Reno, NV) was inserted through a burr hole perforated on the skull into the left lateral ventricle using the following coordinates relative to the bregma: 1 mm lateral, 0.2 mm posterior, and 2.2 mm below the horizontal plane of the bregma. Sterile 2 μL phosphate-buffered saline (PBS; vehicle), polyclonal anti-VEGF antibody (0.2 or 1 μg in 2 μL PBS; AF-493-NA,

R&D System, Minneapolis, MN), polyclonal anti-VEGFR-2 antibody (2 μg in 2 μL PBS; AF644, R&D System, Minneapolis, MN) or nonspecific IgG (1 μg in 2 μL PBS; Abcam, Cambridge, MA) was injected at a rate of 1 μL/min at 30 min post-operation. The dosage of anti-VEGF or anti-VEGFR-2 antibodies was determined based on previous reports [11, 12]. The needle was slowly removed after 5 min of an injection, and the wound was quickly sutured.

Neurobehavioral Test

Neurobehavior functions were blindly assessed using the modified Garcia's neurological score system as previously described [13]. The evaluation consists of six tests that can be scored 0 to 3 or 1 to 3. These six tests include spontaneous activity, spontaneous movement of four limbs, forepaw outstretching, climbing, body proprioception, and response to whisker stimulation (Online Resource, Table S1). Animals were given a total score of 2 to 18 in 1-number steps, and higher scores indicated better function.

SAH Grade

The severity of SAH was blindly evaluated using high-resolution pictures of the base of the brain taken at each sacrifice [10]. The SAH grading system was as follows: the basal cistern was divided into six segments, and each segment was allotted a grade from 0 to 3 depending on the amount of subarachnoid blood clot in the segment; grade 0, no subarachnoid blood; grade 1, minimal subarachnoid blood; grade 2, moderate blood clot with recognizable arteries; and grade 3, blood clot obliterating all arteries within the segment. The animals received a total score ranging from 0 to 18 after adding the scores from all six segments. Mice with SAH grade scores ≤7, which had no significant brain injury, were excluded [10].

Brain Water Content

Brain edema was determined using the wet/dry method as previously described [10]. After sacrificing mice under deep anesthesia, the brain was quickly removed, separated into the left and right cerebral hemispheres, cerebellum, and brain stem, and weighed (wet weight). The brain specimens were dried in an oven at 105 °C for 72 h and weighed again as dry weight. The percentage of water content was calculated according to the following formula: [(wet weight−dry weight)/wet weight]×100 %.

Immunohistochemical Staining

Immunohistochemical staining of IgG was performed to evaluate BBB permeability as previously reported [14]. Under deep anesthesia, mice were sacrificed by intracardial perfusion with 30 mL PBS followed by 15 min of 10 % neutral buffered formalin at 60–80 mmHg. The brains were removed, fixed in 10 % neutral buffered formalin for approximately 12 h at 4 °C and embedded in paraffin. Four-micrometer-thick coronal sections at 1.0 mm posterior to the bregma were cut. After dewaxing and rehydration, the sections were placed in 1 mmol/L ethylenediaminetetraacetic acid (pH 8.0) heating in water bath for 20 min to retrieve antigen. After being incubated in 1 % hydrogen peroxide (H_2O_2) for 10 min to quench any endogenous peroxidase activity, the sections were blocked with 10 % horse serum for 1 h at room temperature followed by overnight incubation at 4 °C with biotinylated horse anti-mouse polyclonal IgG (1:100; Vector Laboratories, Burlingame, CA), and then with an avidin-biotin-horseradish peroxidase complex (Vectastain ABC Kit; Vector Laboratories, Burlingame, CA) for 1 h at room temperature. Color reactions were developed in diaminobenzidine/H_2O_2 solution, and the sections were lightly counterstained with hematoxylin. Four continuous pictures of the left temporal cortex were photographed under light microscope (×20) and the relative quantity of IgG was calculated by Image Pro Plus 6.0 software (Media Cybernetics Inc., Rockville, MD).

Western Blotting

Western blotting was performed as previously described [15]. The left cerebral cortex was separated and used. Equal amounts of protein samples were loaded on SDS-PAGE gels, electrophoresed, and transferred onto a polyvinylidene difluoride membrane. The membranes were blocked with 5 % bovine serum albumin for 2 h at room temperature followed by incubation overnight at 4 °C with polyclonal goat anti-VEGF antibody (0.5 μg/mL; AF-493-NA, R&D System, Minneapolis, MN), polyclonal goat anti-VEGFR-2 antibody (0.5 μg/mL; AF644, R&D System, Minneapolis, MN), monoclonal rabbit anti-p-VEGFR-2 antibody (1:1000; #4991, Cell Signaling Technology, Danvers, MA), polyclonal rabbit anti-zona occludens (ZO)-1 antibody (1:200; 61-7300, Thermo Fisher Scientific, Rockford, IL), polyclonal goat anti-interleukin (IL)-1β antibody (0.25 μg/mL; AF-401-NA, R&D System, Minneapolis, MN) and monoclonal mouse anti-TNC antibody (0.18 μg/mL; 10337, Immuno-Biological Laboratories, Takasaki, Japan). Immunoreactive bands were detected with a chemiluminescence reagent kit (ECL Prime; Amersham Bioscience, Arlington Heights, IL) and quantified by densitometry with Image J software (NIH, Bethesda, MD). β-tubulin (1:1000; sc-9104, Santa Cruz Biotechnology, Santa Cruz, CA) was blotted on the same membrane as a loading control.

Statistical Analysis

Neurological scores and SAH grade were expressed as median±25th–75th percentiles, and were analyzed using Mann-Whitney *U* tests or Kruskal-Wallis tests, followed by Steel-Dwass multiple comparisons. Other values were expressed as mean±standard deviation and one-way analysis of variance (ANOVA) with Tukey-Kramer post hoc test was used. Mortality was compared using chi-square tests. $P<0.05$ was considered significant.

Results

Anti-VEGF Antibody Treatment Ameliorates Neurobehavior and Alleviates Brain Edema After 24 and 48 h of SAH

Comparisons of physiological parameters revealed no significant differences among the groups (data not shown). No sham-operated mice died, and the mortality of SAH mice was not different among vehicle (25.7 %, 9 of 35), 0.2 μg (27.3 %, 3 of 11), and 1 μg (23.5 %, 8 of 34) anti-VEGF antibody treatment groups. Six mice were excluded due to less severe SAH ($n=2$ per group), and in the remaining animals, SAH grade was similar among the 3 SAH groups at 24 h post-operation (Fig. 1a).

Neurological scores were significantly impaired in SAH animals compared with the sham groups at 24 h, and were significantly improved after 1 μg anti-VEGF antibody treatment compared with the SAH+vehicle and SAH+0.2 μg anti-VEGF antibody groups ($P<0.05$, Fig. 1b). Post-SAH brain edema occurred in the left cerebral hemisphere, and was also significantly alleviated after 1 μg anti-VEGF antibody treatment compared with the SAH+vehicle and SAH+0.2 μg anti-VEGF antibody groups ($P<0.05$, Fig. 1c).

Based on the findings in the 24-h study, we eliminated the SAH+0.2 μg anti-VEGF antibody group from the 48-h and the following mechanism studies. At 48 h post-SAH, neurological scores were also significantly aggravated in the SAH+vehicle group compared with the sham+vehicle group, and significantly ameliorated after 1 μg anti-VEGF antibody administration ($P<0.05$, respectively), although the SAH severity was similar (Fig. 2a, b). Post-SAH brain edema in the left cerebral hemisphere was also significantly alleviated after 1 μg anti-VEGF antibody treatment ($P<0.05$, Fig. 2c).

Nonspecific control IgG (16.7 % mortality, 1 of 6) did not show any protective effects (data not shown).

Anti-VEGF Antibody Treatment Prevents BBB Disruption After SAH

The IgG staining results showed that post-SAH BBB disruption significantly occurred in the left cerebral cortex, especially in the temporal lobe (Fig. 3). The IgG extravasation was significantly suppressed after 1 μg anti-VEGF antibody administration compared with the SAH+vehicle group ($P<0.05$; Fig. 3b and c). Western blotting results showed that the expression of the tight junction protein ZO-1 was significantly reduced in the left cerebral cortex in the SAH+vehicle group compared with the sham groups ($P<0.05$; Online Resource, Figure S1). However, the expression of ZO-1 was significantly preserved after 1 μg anti-VEGF antibody treatment compared with the SAH+vehicle group, supporting the protective effects of anti-VEGF antibody against post-SAH BBB disruption ($P<0.05$; Online Resource, Figure S1).

VEGF Neutralization Prevents Post-SAH TNC Induction

Western blotting analyses showed that the expression of VEGF, VEGFR-2 and p-VEGFR-2 was significantly increased in the left cerebral cortex, and was effectively inhibited by the administration of 1 μg anti-VEGF antibody at 24 h post-SAH (Fig. 4). VEGF neutralization and VEGFR-2 inactivation were also associated with the inhibition of post-SAH TNC induction. Anti-VEGF therapy also suppressed a post-SAH increase in IL-1β in the cerebral cortex (Online Resource, Figure S2).

Blockage of VEGFR-2 Suppresses Post-SAH Neurobehavioral Impairments, Brain Edema, and TNC Induction

Comparisons of physiological parameters revealed no significant differences among the groups (data not shown). No sham-operated animals died, and the mortality of SAH mice was 17.6 % (3 of 17 mice) in the both SAH+vehicle and SAH+anti-VEGFR-2 antibody groups. Two mice were excluded from either group due to less severe SAH, and SAH grade in the remaining animals was similar between the 2 SAH groups (Fig. 5a). The anti-VEGFR-2 antibody treatment significantly improved neurological scores and ameliorated brain edema after SAH compared with the SAH+vehicle group ($P<0.05$, respectively; Fig. 5b, c). Anti-VEGFR-2 antibody effectively inhibited the expression of VEGFR-2 and p-VEGFR-2, and downregulated the expression of TNC after SAH compared with the SAH+vehicle group ($P<0.05$, respectively; Fig. 6).

Discussion

In the present study, we first demonstrated that experimental SAH upregulated VEGF expression in the cerebral cortex, causing BBB disruption via VEGFR-2 and at least partly TNC. Both anti-VEGF and VEGFR-2 treatments were effective against post-SAH EBI.

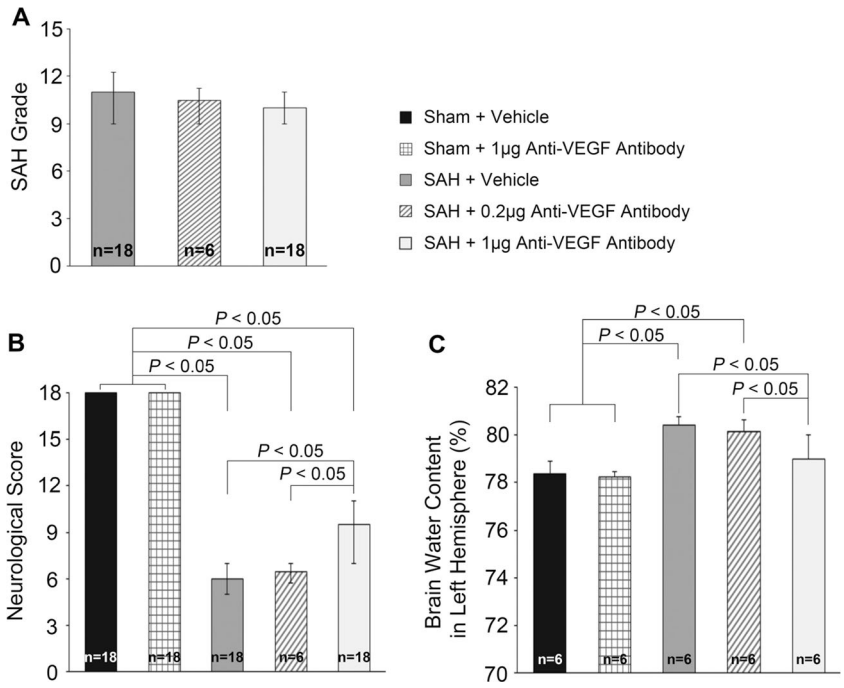

Fig. 1 Effects of anti-vascular endothelial growth factor (*VEGF*) antibody treatment on the severity of subarachnoid hemorrhage (*SAH*; **a**), neurological scores (**b**) and brain water content in the left cerebral hemisphere (**c**) at 24 h post-SAH. Data are expressed as median±25th–75th percentiles (**a**, **b**) and mean±standard deviation (**c**). *P* value, Kruskal-Wallis tests (**a**, **b**) and ANOVA (**c**)

Aneurysmal SAH is a devastating cerebrovascular disease with more than 50 % combined mortality and morbidity rates [16]. EBI is believed to be one of the most important determinants of poor outcome [2]. However, the mechanisms are complex and still indistinct [6, 10, 15]. BBB disruption is known to be an important component of EBI [17, 18]. Enhanced BBB permeability allows inflammatory cytokines and pathological molecules to enter into brain tissue and may cause or aggravate immune reactions and homeostatic imbalance, leading to further brain injuries [1, 2]. Therefore, it may be a reasonable strategy to attenuate EBI by preventing BBB disruption after SAH.

VEGF is a crucial factor of angiogenesis that stimulates vascular permeability under physiological and pathological

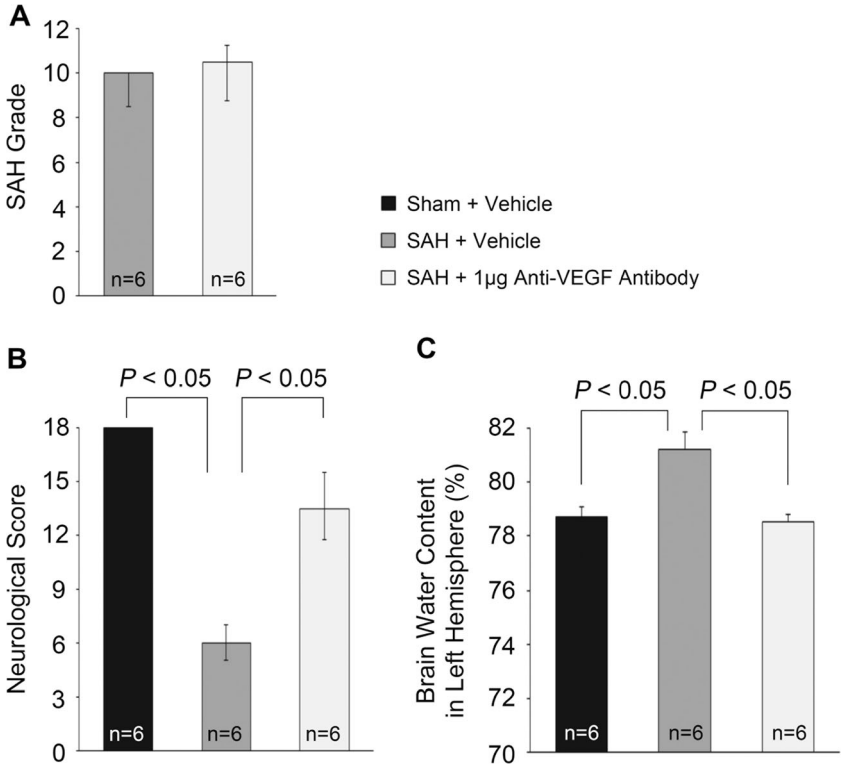

Fig. 2 Effects of anti-vascular endothelial growth factor (*VEGF*) antibody treatment on the severity of subarachnoid hemorrhage (*SAH*; **a**), neurological scores (**b**) and brain water content in the left cerebral hemisphere (**c**) at 48 h post-SAH. Data are expressed as median±25th-75th percentiles (**a**, **b**) and mean±standard deviation (**c**). *P* value, Kruskal-Wallis tests (**a**, **b**) and ANOVA (**c**)

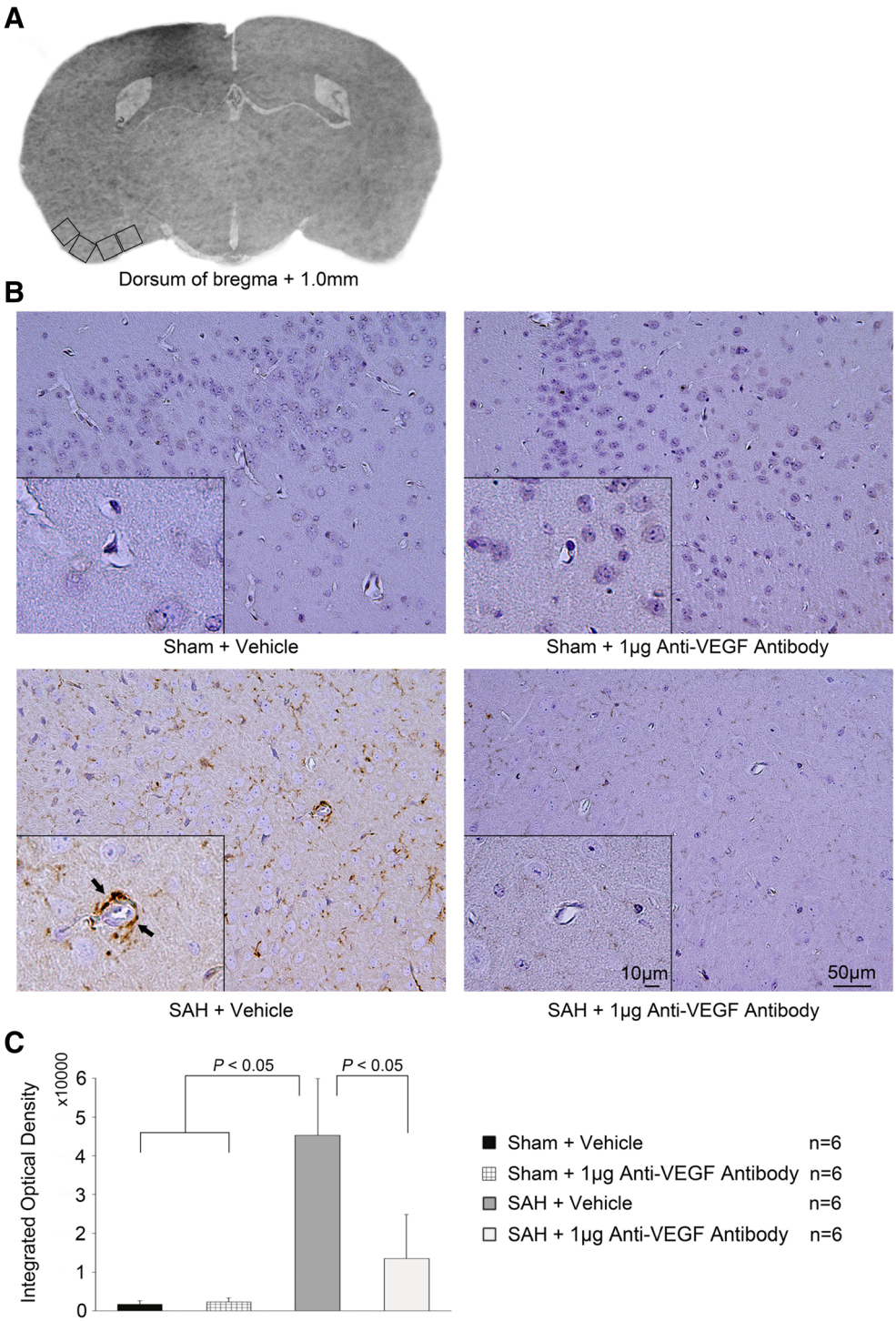

Fig. 3 Effects of anti-vascular endothelial growth factor (*VEGF*) antibody treatment on blood-brain barrier permeability in the left temporal cortex at 24 h after subarachnoid hemorrhage (SAH). Representative SAH brain slice showing four continuous areas of the left temporal cortex (**a**), representative immunoglobulin G (IgG) staining (**b**), and the sum of integrated optical density of IgG (**c**). Data are expressed as mean± standard deviation. *Arrows* extravasated IgG; *P* value, ANOVA

conditions [19]. It has been reported that the expression of VEGF was induced in brain after experimental SAH associated with increased BBB permeability [6, 20, 21]. Some researchers also reported that some drugs or treatments protected post-SAH BBB integrity associated with decreased levels of VEGF in brain, suggesting the pivotal role of VEGF in post-SAH BBB disruption [6, 20–23]. The bioactivity of VEGF is mediated by VEGFR phosphorylation, and there is an agreement that VEGFR-2 is the major mediator of the permeability-enhancing effects of VEGF [3]. Another receptor VEGFR-1 has a very high affinity for VEGF but the kinase activity of about one-tenth that of VEGFR-2, and may negatively regulate VEGFR-2 signaling [24]. Davis et al. [25] demonstrated that VEGF induced VEGFR-2 expression and activated VEGFR-2-mediated downstream signaling to increase BBB permeability in the in vitro BBB model. This

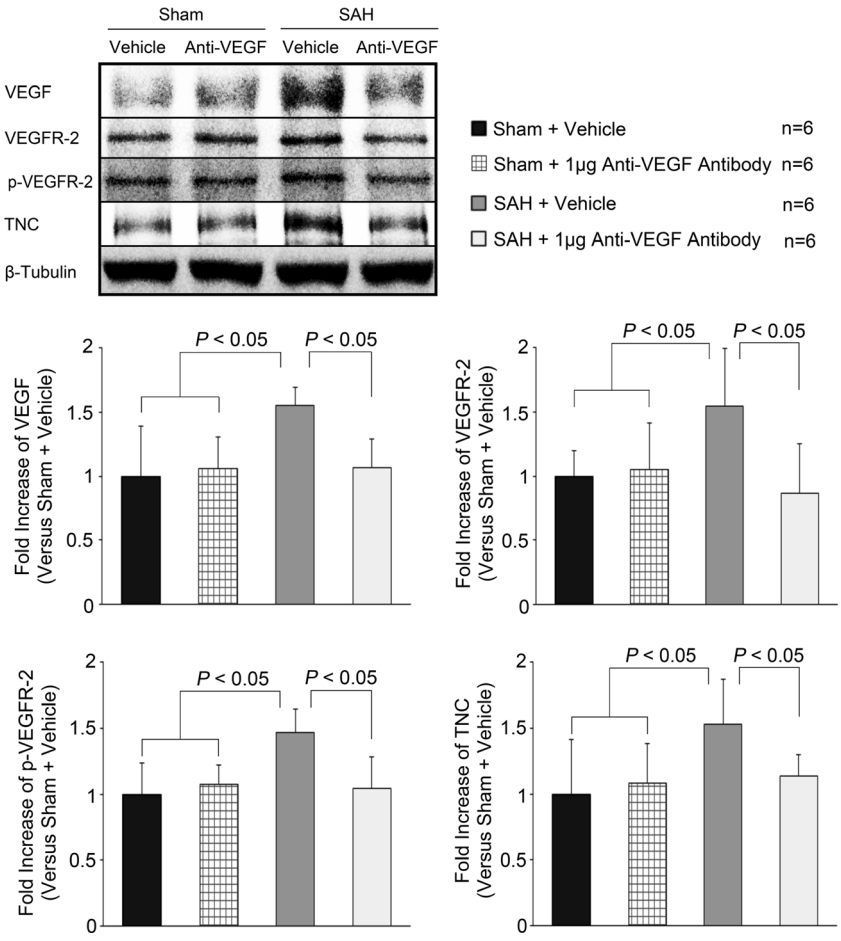

Fig. 4 Representative Western blots and effects of anti-vascular endothelial growth factor (VEGF) antibody treatment on expression of VEGF, VEGF receptor (*VEGFR*)-2, phosphorylated VEGFR-2 (*p-VEGFR-2*), and tenascin-C (*TNC*) in the left cerebral cortex at 24 h after subarachnoid hemorrhage (*SAH*). Expression levels of each protein are expressed as a ratio of β-tubulin levels for normalization and as mean±standard deviation. *P* value, ANOVA

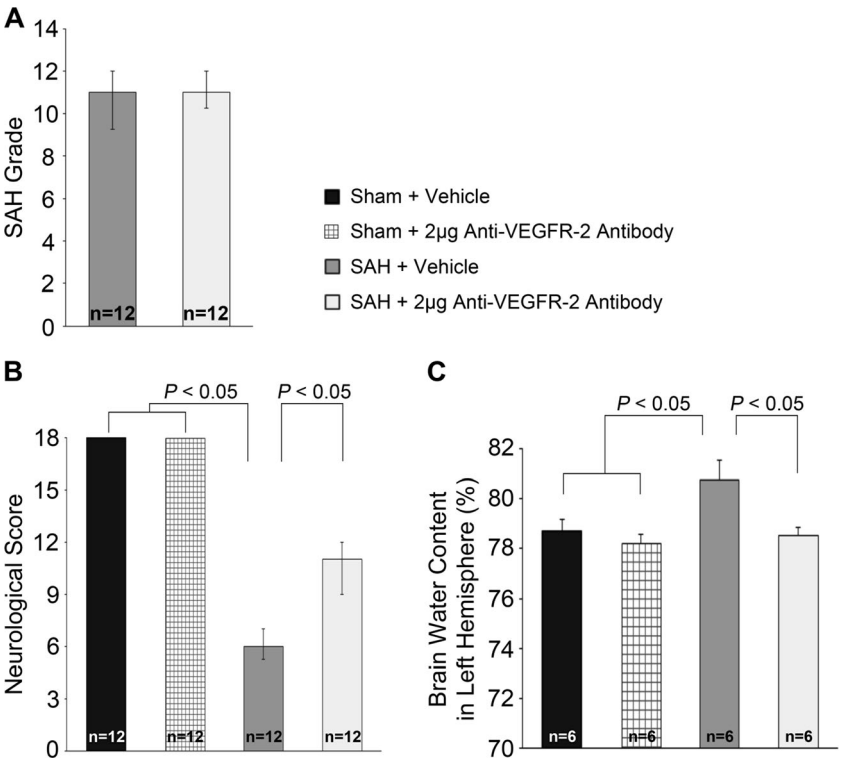

Fig. 5 Effects of anti-vascular endothelial growth factor receptor (*VEGFR*)-2 antibody treatment on the severity of subarachnoid hemorrhage (*SAH*; **a**), neurological scores (**b**) and brain water content in the left cerebral hemisphere (**c**) at 24 h post-SAH. Data are expressed as median± 25th-75th percentiles (**a**, **b**) and mean±standard deviation (**c**). *P* value, Kruskal–Wallis tests (**a**, **b**) and ANOVA (**c**)

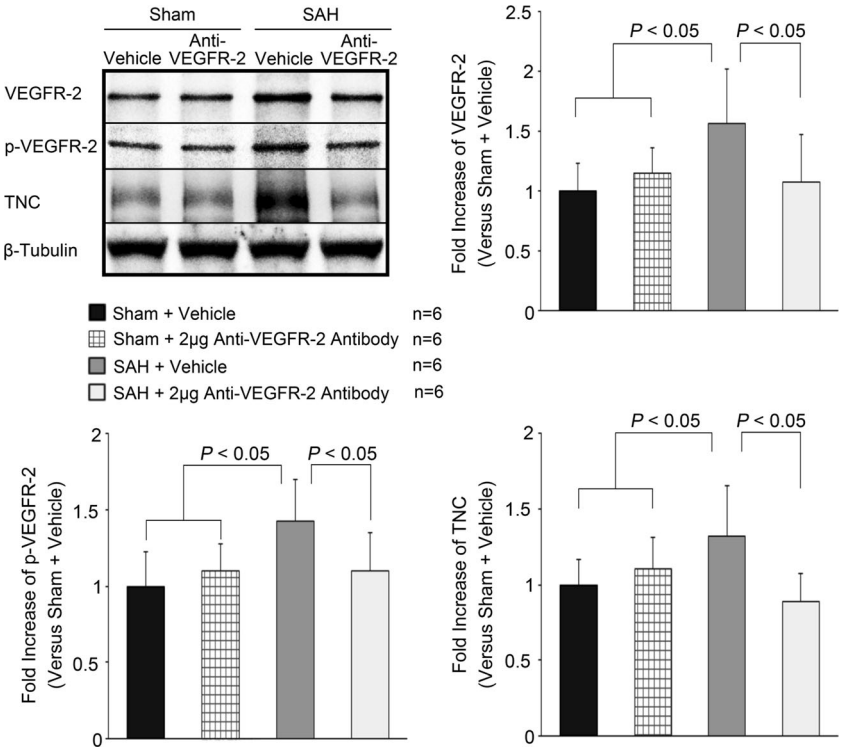

Fig. 6 Representative Western blots and effects of anti-vascular endothelial growth factor receptor (*VEGFR*)-2 antibody treatment on expression of VEGFR-2, phosphorylated VEGFR-2 (*p-VEGFR-2*) and tenascin-C (*TNC*) in the left cerebral cortex at 24 h after subarachnoid hemorrhage (SAH). Expression levels of each protein are expressed as a ratio of β-tubulin levels for normalization and as mean±standard deviation. *P* value, ANOVA

study first showed that a direct blockage of VEGF pathways by anti-VEGF or anti-VEGFR-2 antibodies effectively prevented post-SAH BBB disruption or EBI. It also first indicates that VEGFR-2 is the important receptor that mediates VEGF-induced EBI after SAH.

TNC is a large extracellular matrix glycoprotein that is highly expressed during development, particularly in the nervous system and so on [26]. It is a multi-modular protein comprising four distinct domains: an assembly domain, a series of epidermal growth factor (EGF)-like repeats, a series of fibronectin type III-like repeats, and a C-terminal fibrinogen-like globe, each of which interacts with a different subset of binding partners [26]. Its expression is downregulated in healthy adults and transiently induced during immune response which is caused by tissue injury [27]. On the molecular level, it has been reported that the expression of TNC is induced via MAPK pathways by multiple growth factors, including fibroblast growth factors, platelet-derived growth factors (PDGFs), EGFs, and transforming growth factors [7]. In our previous study, we demonstrated that TNC was upregulated in the cerebral cortex after experimental SAH in rats, and that a PDGF receptor antagonist suppressed TNC induction and attenuated EBI via the inactivation of MAPKs [9]. TNC also induces MAPKs in normal [28] and SAH [9, 29] rats. Although the relationships between TNC and VEGF have never been studied in SAH brain, TNC regulates VEGF expression in tumor [30]. To the best of our knowledge, there are no studies reporting that VEGF induces TNC. However, as MAPK may have a significant role in BBB disruption as both upstream and downstream of VEGF [6], it may be reasonable to consider that TNC and VEGF may interact via MAPKs and affect the BBB integrity. Our recent study also demonstrated that the expression of TNC is the upstream of BBB disruption after SAH using TNC knockout mice [31]. Taken together, this study first showed that VEGF-induced post-SAH BBB disruption might be mediated at least partly by TNC's action.

Another interesting finding in this study is that anti-VEGF antibody downregulated VEGFR-2. VEGF bound to the neutralizing antibody is no longer detected on the Western blot using the same antibody, and loses the biological effects, leading to inactivation of the receptor VEGFR-2 and the downstream signaling MAPKs [6]. As a result, anti-VEGF neutralizing antibody possibly downregulated VEGFR-2, as VEGF was reported to upregulate VEGFR-2 through MAPKs [32]. Neutralizing VEGF might also downregulate VEGFR-2 via inhibiting TNC expression, as TNC is known to upregulate multiple receptors [28, 29]. As well, anti-VEGFR-2 neutralizing antibody should block the biological effects of VEGFR-2, that is, the activity, and might suppress MAPKs, leading to VEGFR-2 downregulation. Thus, the ratio of p-VEGFR-2/total VEGFR-2 was similar among groups in this study, which is consistent with a previous study [25]. In addition, this study showed that anti-VEGF therapy suppressed a post-SAH increase in a pro-inflammatory cytokine IL-1β in the cerebral cortex, which is involved in post-SAH BBB disruption [33]. IL-1β suppression might also contribute to anti-VEGF therapy's protective effects against post-SAH BBB disruption. IL-1β may induce TNC production by MAPK-dependent or

MAPK-independent pathways [34], while TNC may stimulate synthesis of IL-1β [35]. The positive feedback mechanisms between TNC and IL-1β may cause post-SAH BBB disruption.

The efficacy and safety of anti-VEGF therapy have recently been proved by various clinical trials as to the normalization of abnormally permeable tumor vessels [36] or the suppression of blood-retinal barrier breakdown [37]. We demonstrated for the first time that anti-VEGF treatment prevented EBI after SAH via inhibiting the upregulation of TNC in this study. However, the antibodies were given via an intracerebroventricular injection at 30 min post-SAH, and this diminishes the translational significance of the study. When considering the pathophysiology of post-SAH EBI, earlier administration of the antibodies would result in better outcome, but no data is available about it. The effects of other administration methods, multiple treatments at different dosages or time courses, therapeutic time window as well as long-term functional outcomes should be examined before clinical trials. Anti-VEGF or VEGFR-2 treatments are promising as a new therapy against post-SAH EBI, and our findings warrant more research.

Acknowledgments We thank Ms. Chiduru Yamamoto (Department of Neurosurgery, Mie University Graduate School of Medicine) for her technical assistance. This work was supported by a Grant-in-Aid for Scientific Research from Mie University Hospital Seed Grant Program 2014 to Dr. Suzuki, and Japan Society for the Promotion of Science to Dr. Fujimoto.

Conflict of Interest The authors declare that they have no conflict of interest.

Research Involving Animals All procedures were approved by the Animal Ethics Review Committee of Mie University, and were carried out according to the institution's Guidelines for Animal Experiments.

Funding This work was funded by a Grant-in-Aid for Scientific Research from Mie University Hospital Seed Grant Program 2014 to Dr. Suzuki, and Japan Society for the Promotion of Science to Dr. Fujimoto.

References

1. Cahill J, Calvert JW, Zhang JH (2006) Mechanisms of early brain injury after subarachnoid hemorrhage. J Cereb Blood Flow Metab 26:1341–1353
2. Fujii M, Yan J, Rolland WB et al (2013) Early brain injury, an evolving frontier in subarachnoid hemorrhage research. Transl Stroke Res 4:432–446
3. Ferrara N, Gerber HP, LeCouter J (2003) The biology of VEGF and its receptors. Nat Med 9:669–676
4. Jiang S, Xia R, Jiang Y et al (2014) Vascular endothelial growth factors enhance the permeability of the mouse blood-brain barrier. PLoS One 9:e86407
5. Argaw AT, Asp L, Zhang J et al (2012) Astrocyte-derived VEGF-A drives blood-brain barrier disruption in CNS inflammatory disease. J Clin Invest 122:2454–2468
6. Kusaka G, Ishikawa M, Nanda A et al (2004) Signaling pathways for early brain injury after subarachnoid hemorrhage. J Cereb Blood Flow Metab 24:916–925
7. Tucker RP, Chiquet-Ehrismann R (2009) The regulation of tenascin expression by tissue microenvironments. Biochim Biophys Acta 1793:888–892
8. Suzuki H, Kanamaru K, Shiba M et al (2011) Cerebrospinal fluid tenascin-C in cerebral vasospasm after aneurysmal subarachnoid hemorrhage. J Neurosurg Anesthesiol 23:310–317
9. Shiba M, Fujimoto M, Imanaka-Yoshida K et al (2014) Tenascin-C causes neuronal apoptosis after subarachnoid hemorrhage in rats. Transl Stroke Res 5:238–247
10. Altay O, Suzuki H, Hasegawa Y et al (2012) Isoflurane attenuates blood-brain barrier disruption in ipsilateral hemisphere after subarachnoid hemorrhage in mice. Stroke 43:2513–2516
11. Chi OZ, Hunter C, Liu X et al (2007) Effects of anti-VEGF antibody on blood-brain barrier disruption in focal cerebral ischemia. Exp Neurol 204:283–287
12. Krum JM, Mani N, Rosenstein JM (2008) Roles of the endogenous VEGF receptors flt-1 and flk-1 in astroglial and vascular remodeling after brain injury. Exp Neurol 212:108–117
13. Suzuki H, Zhang JH (2012) Neurobehavioral assessments of subarachnoid hemorrhage. In: Chen J, Xu X-M, Xu ZC, Zhang JH (eds) Springer protocols handbooks. Animal models of acute neurological injuries II. Humana, New York, pp 435–440
14. Richmon JD, Fukuda K, Maida N et al (1998) Induction of heme oxygenase-1 after hyperosmotic opening of the blood-brain barrier. Brain Res 780:108–118
15. Suzuki H, Ayer R, Sugawara T et al (2010) Protective effects of recombinant osteopontin on early brain injury after subarachnoid hemorrhage in rats. Crit Care Med 38:612–618
16. Zacharia BE, Hickman ZL, Grobelny BT et al (2010) Epidemiology of aneurysmal subarachnoid hemorrhage. Neurosurg Clin N Am 21:221–233
17. Friedrich V, Flores R, Muller A et al (2010) Escape of intraluminal platelets into brain parenchyma after subarachnoid hemorrhage. Neuroscience 165:968–975
18. Scholler K, Trinkl A, Klopotowski M et al (2007) Characterization of microvascular basal lamina damage and blood-brain barrier dysfunction following subarachnoid hemorrhage in rats. Brain Res 1142:237–246
19. Takahashi H, Shibuya M (2005) The vascular endothelial growth factor (VEGF)/VEGF receptor system and its role under physiological and pathological conditions. Clin Sci 109:227–241
20. Ostrowski RP, Colohan AR, Zhang JH (2005) Mechanisms of hyperbaric oxygen-induced neuroprotection in a rat model of subarachnoid hemorrhage. J Cereb Blood Flow Metab 25:554–571
21. Suzuki H, Hasegawa Y, Kanamaru K et al (2010) Mechanisms of osteopontin-induced stabilization of blood-brain barrier disruption after subarachnoid hemorrhage in rats. Stroke 41:1783–1790
22. Yatsushige H, Ostrowski RP, Tsubokawa T et al (2007) Role of c-Jun N-terminal kinase in early brain injury after subarachnoid hemorrhage. J Neurosci Res 85:1436–1448
23. Zhang J, Xu X, Zhou D et al (2014) Possible role of Raf-1 kinase in the development of cerebral vasospasm and early brain injury after experimental subarachnoid hemorrhage in rats. Mol Neurobiol. doi: 10.1007/s12035-014-8939-7
24. Shibuya M (2013) Vascular endothelial growth factor and its receptor system: physiological functions in angiogenesis and pathological roles in various diseases. J Biochem 153:13–19
25. Davis B, Tang J, Zhang L et al (2010) Role of vasodilator stimulated phosphoprotein in VEGF induced blood-brain barrier permeability in endothelial cell monolayers. Int J Dev Neurosci 28:423–428
26. Midwood KS, Hussenet T, Langlois B et al (2011) Advances in tenascin-C biology. Cell Mol Life Sci 68:3175–3199

27. Udalova IA, Ruhmann M, Thomson SJ et al (2011) Expression and immune function of tenascin-C. Crit Rev Immunol 31:115–145
28. Fujimoto M, Suzuki H, Shiba M et al (2013) Tenascin-C induces prolonged constriction of cerebral arteries in rats. Neurobiol Dis 55: 104–109
29. Shiba M, Suzuki H, Fujimoto M et al (2012) Imatinib mesylate prevents cerebral vasospasm after subarachnoid hemorrhage via inhibiting tenascin-C expression in rats. Neurobiol Dis 46:172–179
30. Tanaka K, Hiraiwa N, Hashimoto H et al (2004) Tenascin-C regulates angiogenesis in tumor through the regulation of vascular endothelial growth factor expression. Int J Cancer 108:31–40
31. Fujimoto M, Shiba M, Kawakita F et al. (2015) Deficiency of tenascin-C attenuates blood-brain barrier disruption after experimental subarachnoid hemorrhage in mice. J Neurosurg. In press
32. Li W, Lu ZF, Man XY et al (2012) VEGF upregulates VEGF receptor-2 on human outer root sheath cells and stimulates proliferation through ERK pathway. Mol Biol Rep 39:8687–8694
33. Sozen T, Tsuchiyama R, Hasegawa Y et al (2009) Role of interleukin-1beta in early brain injury after subarachnoid hemorrhage in mice. Stroke 40:2519–2525
34. Chiquet-Ehrismann R, Chiquet M (2003) Tenascins: regulation and putative functions during pathological stress. J Pathol 200:488–499
35. Kuriyama N, Duarte S, Hamada T et al (2011) Tenascin-C: a novel mediator of hepatic ischemia and reperfusion injury. Hepatology 54:2125–2136
36. Narita Y (2013) Drug review: safety and efficacy of bevacizumab for glioblastoma and other brain tumors. Jpn J Clin Oncol 43:587–595
37. Stefanini FR, Badaro E, Falabella P et al (2014) Anti-VEGF for the management of diabetic macular edema. J Immunol Res 2014: 632307